Open Access

Iraqi Journal of Industrial Research (IJOIR)

Journal homepage: http://ijoir.gov.iq

Fuel Consumption Reduction and Energy Efficiency Enhancement in Allyl Chloride Production through Heat Recovery and Steam Integration Strategies

Farrel Dzakwan Alghiffary*

Department of Chemical Engineering, Faculty of Engineering, Diponegoro University, Semarang, Indonesia

Article information

Article history:
Received: February, 19, 2026
Accepted: May, 24, 2026
Available online: June, 14, 2026

Keywords:
Allyl chloride,
Process modification,
Fuel reduction,
Energy efficiency

Corresponding Author:
Farrel Dzakwan Alghiffary
farreldzakwan.ldtk1@gmail.com

DOI:
https://doi.org/10.53523/ijoirVol13I1ID651

Abstract

Allyl chloride production via high temperature propylene chlorination (HTPC) is a strongly exothermic process operating at 420–510 °C and generating substantial recoverable thermal energy in the reactor effluent. In conventional configurations, a significant portion of this high-grade heat is dissipated, while external fuel combustion and steam utilities are required to maintain reactor inlet temperature and downstream heating. This study proposes a systematic heat integration strategy that simultaneously utilizes reactor effluent heat for feed preheating and internal steam generation, providing a more effective approach to reduce overall energy demand. Process simulations were performed using Aspen HYSYS based on rigorous mass and energy balances to evaluate both base and modified configurations, employing the Cubic-Plus-Association (CPA) equation of state due to its improved accuracy in representing non-ideal mixtures containing polar and associating components commonly found in chlorination systems. In the integrated design, reactor effluent heat was utilized to preheat the propylene feed to 200 °C and to generate 6 bar saturated steam for internal process heating. The results show a furnace duty reduction of 5.38×10^6 kJ/h (≈26.3%), corresponding to fuel savings of 228.27 kg/h (≈26.3%) and a carbon dioxide (CO_2) emission reduction of 626.20 kg/h (≈26.3%). Additionally, 1.3943×10^7 kJ/h of thermal energy was recovered. The economic evaluation, based on reduced natural gas consumption and elimination of external steam requirements, indicates significant operational cost savings and practical feasibility for industrial implementation.

1. Introduction

Allyl chloride is a crucial petrochemical intermediate with significant industrial and economic importance. The global market value of allyl chloride is projected to reach USD 5.02 billion by 2030 [1], reflecting its expanding role in downstream chemical industries. This compound is primarily utilized in the production of major organic intermediates such as epichlorohydrin (ECH), glycerol, and allyl alcohol. Industrially, more than 80% of epichlorohydrin is produced from allyl chloride, and one of the principal applications of ECH is in epoxy resin

manufacturing, for which global demand reached 5.19 million tons in 2016 [2]. Compared with the conventional chlorohydrin process for ECH production, the direct epoxidation of allyl chloride offers a simpler process configuration and substantially reduced wastewater generation, making it a more environmentally favorable alternative [3]. Beyond epichlorohydrin, allyl chloride is also used in the manufacture of glycidyl esters, polymers, plastics, pharmaceuticals, protective coatings, elastomers, pesticides, detergents, sealants, and other allylic derivatives, demonstrating its versatility across diverse chemical sectors [4]. In 2022, the global market value of allyl chloride was estimated at approximately USD 2,014.54 million, with an expected annual growth rate between 5.00% and 6.72% during the current decade [5].

The increasing global demand for allyl chloride has intensified the need for efficient and economically sustainable production technologies. Currently, industrial synthesis mainly relies on high-temperature propylene chlorination (HTPC) and propylene oxychlorination, with HTPC remaining the predominant route due to its relatively simple process configuration and lower capital investment, as it does not require a catalyst [2]. In contrast, the oxychlorination process requires noble metal catalysts that are susceptible to deactivation. Despite its advantages, the high-temperature chlorination of propylene is characterized by rapid reaction kinetics and strongly exothermic behavior [3]. Industrial operation is typically conducted within a temperature range of approximately 420–510 °C to achieve favorable conversion and selectivity [6].

The elevated operating temperature range of 420–510 °C in the high-temperature chlorination of propylene inevitably results in substantial thermal energy within the reactor effluent stream. While the exothermic nature of the reaction contributes to maintaining reaction temperature, external heating through a furnace is still required to preheat the reactants to the desired inlet conditions. Consequently, significant fuel consumption is associated with maintaining steady reactor operation. Without proper thermal integration, a considerable portion of the high-grade heat contained in the reactor outlet stream is dissipated, leading to inefficiencies in overall energy utilization [7].Effective heat management therefore becomes a critical aspect of process optimization, particularly in large-scale industrial operations where energy demand directly influences production costs and environmental performance [8].

To address these challenges, waste heat recovery strategies can be implemented to utilize the thermal energy of the reactor effluent for feed preheating and utility generation. Previous studies on heat integration have primarily focused on general energy recovery approaches or single heat utilization pathways, with limited attention to the simultaneous application of reactor effluent heat for both feed preheating and steam generation in allyl chloride production under HTPC conditions. In addition, quantitative evaluations of the impact of such integrated strategies on furnace duty, fuel consumption, and emission reduction remain relatively scarce. Therefore, a clear need exists for a systematic assessment of integrated heat recovery configurations that can maximize energy utilization in this process. In this study, a combined heat integration strategy is proposed, in which reactor effluent heat is utilized simultaneously for propylene feed preheating and saturated steam generation. The process is evaluated through rigorous simulation to quantify its impact on energy efficiency, fuel consumption, and environmental performance. This work provides a more comprehensive understanding of heat recovery potential in HTPC systems and demonstrates a practical approach to improving the thermal and economic performance of industrial allyl chloride production.

2. Methods

2.1. Allyl Chloride Production

Allyl chloride is industrially produced mainly through two established routes: high-temperature propylene chlorination (HTPC) and propylene oxychlorination (OP). Among these alternatives, HTPC is more widely implemented due to its simpler configuration and lower capital investment, as it does not require catalytic materials [9]. In contrast, the oxychlorination route depends on catalysts that are susceptible to deactivation, thereby increasing operational complexity and cost. Consequently, gas-phase chlorination of propylene remains the dominant industrial technology. In this process, vapor-phase propylene reacts with chlorine via a free-radical mechanism to produce allyl chloride as the principal product and hydrogen chloride as a by-product [2].

The chlorination reaction occurs in the gas phase within a temperature range of 420–510 °C, where elevated temperatures enhance reaction rates and promote allyl chloride formation. Industrial operation involves rapid mixing of vapor-phase propylene and chlorine followed by reaction at pressures of 69–240 kPa and short residence times of 1–4 s to achieve high chlorine conversion [10]. Due to the strongly exothermic nature of the reaction, the system is typically operated under near-adiabatic conditions, resulting in a temperature rise along the reactor. However, reactor temperature must be controlled below 510 °C to prevent pyrolysis, coke formation, and reduced selectivity. Therefore, proper thermal management is essential to ensure stable operation and optimal product yield. The principal and secondary reaction pathways are summarized in Table (1) [11, 12].

Table (1): Kinetic & thermodynamic of primary and secondary reactions in allyl chloride synthesis.

Reaction	A ($kmol/m^3.s$)	Ea (kJ/mol)	ΔH^0_{298K} (kJ/mol)
Allyl chloride formation $C_3H_6 + Cl_2 \rightarrow C_3H_5Cl + HCl$	3.22×10^{-1}	63.200	-112
2-chloropropene (isomer) formation $C_3H_6 + Cl_2 \rightarrow C_3H_5Cl + HCl$	1.83×10^{-5}	16.000	-121
Dichloropropene formation $C_3H_6 + 2Cl_2 \rightarrow C_3H_4Cl_2 + 2HCl$	1.27×10^{-3}	72.100	-306

Another critical and interdependent design variable is the chlorine-to-propylene molar ratio. Propylene is typically supplied in excess, functioning not only as a reactant but also as a diluent and thermal sink that absorbs the heat released from the strongly exothermic reaction, thereby minimizing the formation of by-products [10]. Ratios in the range of 2–6 have been investigated, while industrial practice commonly adopts values between 4 and 6 to achieve favorable selectivity and technical performance [2, 10]. However, excessive propylene increases recycle load, compression duty, and equipment size, thus elevating both capital and operating costs. Therefore, an optimal balance between conversion, selectivity, and economic performance must be achieved through proper adjustment of the reactant ratio.

The conceptual design employed in this study is based on the allyl chloride plant configuration introduced by Turton *et al*. [12] and further developed in subsequent studies [9]. The process consists of a high-temperature reactor followed by heat recovery and multi-stage separation to obtain high-purity allyl chloride. Process simulation was carried out in Aspen HYSYS V11 using the Cubic-Plus-Association (CPA) equation of state, which integrates the Soave–Redlich–Kwong (SRK) framework with an association term to account for specific intermolecular interactions [13]. This model was selected due to its improved capability in representing non-ideal mixtures containing polar and associating components commonly found in chlorination systems. The association term, based on Wertheim's perturbation theory, enhances the accuracy of phase behavior prediction, thereby supporting reliable process simulation and heat integration analysis [14].

2.2. Energy Integration Strategy

The energy integration strategy implemented in this study aims to maximize internal heat recovery from the high-temperature reactor effluent in order to reduce external fuel consumption and improve overall thermal efficiency. The allyl chloride chlorination reactor operates at approximately 510 °C and generates a substantial amount of recoverable thermal energy due to the highly exothermic nature of the reaction. In conventional configurations, this heat is typically removed using cooling utilities prior to downstream separation, leading to inefficient energy utilization. To address this limitation, a systematic heat integration scheme was developed and evaluated using Aspen HYSYS simulation.

A steady-state model of the allyl chloride production process was constructed in Aspen HYSYS to represent both the base configuration and the heat-integrated design. The integration approach is based on fundamental heat recovery principles, in which high-temperature streams are utilized to supply heat to colder process streams before

external utilities are introduced. In the proposed configuration, the reactor effluent at 510 °C is first directed to a heat exchanger, where its thermal energy is used to preheat the propylene feed stream to approximately 200 °C before entering the fired heater. This reduces the required furnace duty while maintaining the same reactor inlet conditions.

Following this step, the reactor effluent still retains considerable residual heat. The partially cooled stream is subsequently routed to a waste heat boiler, where additional heat recovery is achieved through saturated steam generation at 6 bar. The generated steam is then utilized to heat the overhead stream from the first distillation column prior to adsorption, increasing its temperature to approximately 30 °C. This sequential utilization of thermal energy reflects a heat cascade approach, where energy is recovered across multiple temperature levels to maximize efficiency. Although a formal optimization algorithm is not applied, the proposed configuration is systematically designed based on thermodynamic principles to enhance energy utilization and reduce external utility demand.

3. Results and Discussion

3.1. Comparison between Basic and Modified Processes

The simulations of both the unmodified and modified allyl chloride production processes developed using Aspen HYSYS are presented in Figures (1 & 2). The Aspen HYSYS simulation model of the unmodified configuration is presented in Figure (1). In this conventional scheme, the reactor effluent exiting at approximately 510 °C is cooled directly using external cooling utilities prior to downstream separation. The substantial thermal energy released by the highly exothermic chlorination reaction is not internally recovered. Consequently, the propylene feed must be heated primarily by the fired heater to achieve the required reactor inlet temperature, resulting in higher fuel consumption and utility demand.

In contrast, the Aspen HYSYS simulation of the modified process is shown in Figure (2). In this configuration, the reactor effluent at 510 °C is first routed to a heat exchanger to preheat the propylene feed to approximately 200 °C before entering the furnace. This temperature was selected to maximize heat recovery while maintaining a safe margin below the reaction temperature, thereby preventing premature reaction or thermal degradation. In addition, this range ensures effective heat transfer performance within typical shell and tube heat exchanger operating limits, avoiding excessive fouling and maintaining a sufficient temperature driving force for efficient energy exchange [15]. The partially cooled effluent is then directed to a waste heat boiler to generate saturated steam at 6 bar. The internally generated steam is subsequently utilized to heat the overhead stream from the first distillation column prior to entering the adsorption unit, thereby recovering both high- and medium-grade thermal energy within the process.

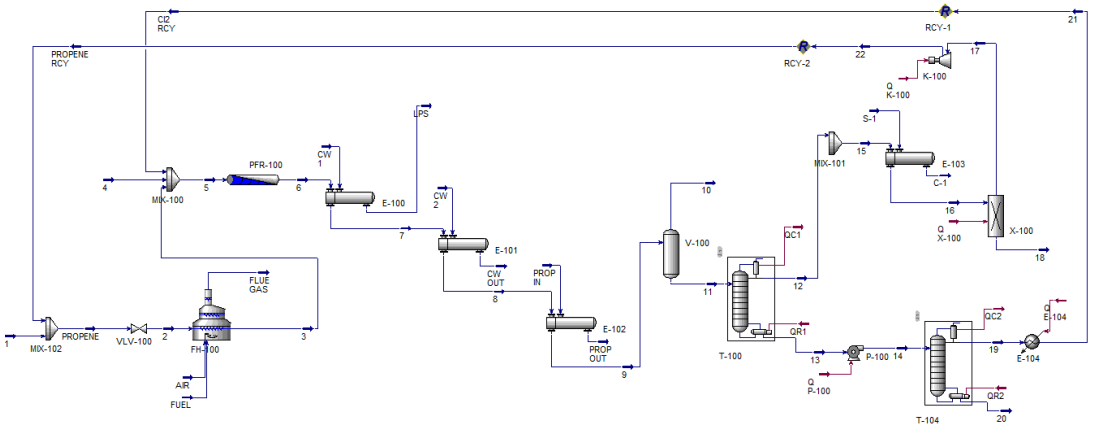

Figure (1): Simulation using Aspen HYSYS of basic (unmodified) process.

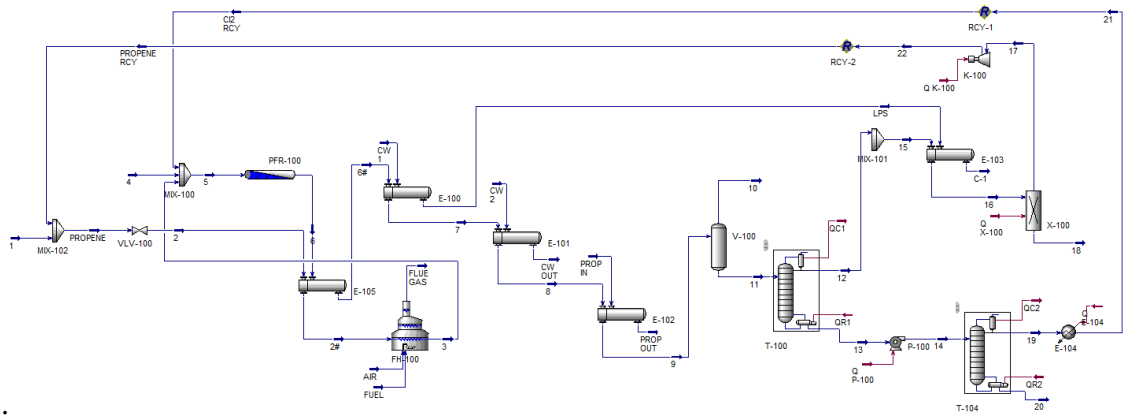

Figure (2): Aspen HYSYS simulation of the heat-integrated (modified) process, showing feed preheating before the furnace and steam generation from reactor effluent.

The primary distinction between the two configurations lies in the degree of energy integration. In the unmodified process, the heat released from the reactor is largely rejected to the environment, and external utilities are relied upon for feed heating and downstream thermal requirements. Conversely, the modified configuration systematically redistributes the exothermic energy of reaction for feed preheating and steam generation, reducing dependence on external fuel and steam utilities. Although the reaction and separation sequence remains unchanged, the modified design fundamentally restructures the internal energy flow, resulting in improved thermal efficiency without altering production capacity.

3.2. Furnace Fuel Consumption Reduction

The reduction in furnace fuel consumption achieved through the proposed heat integration strategy is summarized in Table (2). In the baseline configuration, the fired heater (FH-100) requires 867.735 kg/h of fuel and 26007.784 kg/h of combustion air to reach the desired reactor inlet temperature. Under these operating conditions, 2380.431 kg/h of CO_2 is produced, and the overall thermal duty amounts to 2.046×10^7 kJ/h. From a thermodynamic standpoint, the duty of a fired heater is directly linked to the enthalpy rise of the process stream, which depends on the temperature difference and the heat capacity of the feed. Without internal heat recovery, the entire enthalpy requirement must be supplied by combustion, leading to higher fuel demand and increased greenhouse gas emissions.

Table (2): Summary of fuel, air, CO_2 generation, and energy savings in FH-100.

Parameter	Unit	Unmodified	Modified	Saving	Saving (%)
Fuel	kg/h	867.735	639.469	228.266	26.31
Air	kg/h	26007.784	19166.176	6841.608	26.31
CO_2 generation	kg/h	2380.431	1754.235	626.196	26.31
Overall Performance	kJ/h	2.046×10^7	1.508×10^7	5.38×10^6	26.31

In the modified configuration, the integration of reactor effluent heat recovery substantially reduces the furnace thermal load. As presented in Table (2), fuel consumption decreases to 639.469 kg/h, while air demand drops to 19166.176 kg/h. Consequently, CO_2 generation declines to 1754.235 kg/h, and the overall furnace duty is reduced to 1.508×10^7 kJ/h. Based on energy balance principles, any increase in feed preheating temperature lowers the additional enthalpy required from combustion, thereby proportionally reducing fuel consumption [16]. This behavior is consistent with classical fired heater performance theory, in which enhanced upstream heat recovery directly decreases firing rates and stack losses.

Overall, the modification results in a fuel saving of 228.266 kg/h and an air saving of 6841.608 kg/h, accompanied by a CO_2 reduction of 626.196 kg/h. The total energy saving achieved is 5.38×10^6 kJ/h, representing a significant decrease in external energy input. From a process integration perspective, this outcome illustrates the principle of heat cascade utilization, whereby high-temperature streams are employed to meet upstream heating requirements before external utilities are introduced. By reducing reliance on combustion energy, the modified configuration not only enhances thermal efficiency but also improves environmental performance through lower carbon emissions. These findings demonstrate that strategic internal heat recovery can effectively optimize furnace operation without compromising process stability or production capacity.

3.3. Steam Utilization and Internal Heat Recovery

The residual heat from the reactor effluent is further harnessed for low-pressure steam (LPS) generation, as summarized in Table (3). The recovered steam operates at 6 bar with a saturation temperature of 158.9 °C, corresponding to a molar flow rate of 244.7 kmol/h and a mass flow rate of 4408 kg/h. Converting sensible heat from a high-temperature stream into saturated steam represents a classical waste heat recovery strategy in process engineering. In line with heat integration principles, thermal energy from hot process streams should be utilized internally before being rejected to cooling utilities, thereby improving overall thermal efficiency and reducing external utility demand [17]. By transforming excess reactor heat into usable steam, the process effectively upgrades medium-grade thermal energy into a flexible heating utility.

Table (3): Low pressure steam specification generated from waste heat recovery.

LPS Specification	
Pressure (bar)	6
Temperature (C)	158.9
Molar flow (kmol/h)	244.7
Mass flow (kg/h)	4408

The impact of steam recovery on process heating requirements is presented in Table (4). In the baseline configuration, E-100 and E-103 require external heating duties of 1.675×10^7 kJ/h and 8.573×10^6 kJ/h, respectively. Following modification, the duty of E-100 decreases to 1.138×10^7 kJ/h, yielding an energy saving of 5.37×10^6 kJ/h, while the heating demand of E-103 is fully met by internally generated LPS. This outcome can be explained by the first law of thermodynamics, which states that the required utility duty is proportional to the enthalpy rise of the process stream [18]. When internal heat is supplied through recovered steam, the need for external steam generation is correspondingly reduced.

Table (4): Heat duty reduction and total energy savings from steam utilization.

Unit	Unmodified	Modified	Saving
E-100 Duty (kJ/h)	1.675×10^7	1.138×10^7	5.37×10^6
E-103 Duty (kJ/h)	8.573×10^6	(use LPS from E-100)	8.573×10^6
Total energy saving (kJ/h)			1.3943×10^7

The total energy saving achieved through steam utilization reaches 1.3943×10^7 kJ/h, as shown in Table (4). Effective heat recovery requires appropriate temperature matching between the heat source and the heat sink, a principle emphasized in pinch analysis methodology. The selection of 6 bar steam ensures a sufficient temperature driving force to heat the distillation overhead stream to 30 °C without introducing excessive irreversibility. By integrating steam generation within the process rather than relying on external utilities, the modified configuration enhances thermal efficiency while simultaneously reducing operational costs and environmental impact. These

results demonstrate that systematic internal heat recovery can significantly improve energy performance without altering the core reaction and separation sequence.

3.4. Cost Savings from Heat Integration

Table (5) presents the economic impact of fuel consumption reduction in the fired heater FH-100 after implementing heat integration. The furnace utilizes natural gas with a market price of 3.1048 $/MMBtu obtained from [19], which is equivalent to approximately 0.147 $/kg after unit conversion based on its heating value. Since furnace operating cost is directly proportional to fuel flowrate, any reduction in heat duty directly decreases fuel consumption. In the modified configuration, fuel usage decreases by 228.266 kg/h, resulting in an operational cost saving of 33.555 $/h. According to the first law of thermodynamics, lowering external heat demand reduces the chemical energy required from combustion, thereby decreasing fuel input proportionally [20]. Therefore, the savings observed in Table (5) are a direct consequence of improved thermal efficiency achieved through internal heat recovery.

Table (5): Economic impact of fuel reduction in FH-100.

Data	Value
Fuel type	Natural Gas
Fuel cost ($/kg)	0.147
Fuel Saving (kg/h)	228.266
Cost Saving ($/h)	33.555

The reduction in fuel demand is consistent with combustion system theory, where the required fuel flowrate is determined by the ratio between process heat duty and furnace efficiency. When part of the process heating requirement is satisfied internally, the firing rate of the furnace decreases accordingly. This reduction not only lowers fuel consumption but also decreases air requirement and flue gas generation, leading to both economic and environmental benefits [21]. Because fuel expenses typically represent a significant fraction of total operating cost in petrochemical facilities, minimizing furnace duty provides strong economic justification for heat integration. The data in Table (5) clearly demonstrate that the modified process improves operational efficiency while generating measurable financial savings.

Table (6): Estimation of steam generation cost for unit E-103 in the unmodified process.

Calculation of steam cost			
Fuel type		Natural Gas	
Fuel cost	aF	3.1048	$/MMBtu
Enthalpy of steam	Hs	1188.03	Btu/lb
Enthalpy of boiler feedwater	hw	36.1	Btu/lb
Boiler efficiency	η_B	0.8	
Fuel cost	CF	4.47	$/1000lb
Steam cost	CG	5.81	$/1000lb

Table (6) presents the estimation of steam production cost using the boiler cost correlation reported in [22], which is derived from an overall energy balance around the boiler. The fuel cost component for steam generation is calculated using:

$$C_F = a_F \times \frac{H_s - h_w}{1000\eta_B} \qquad (1)$$

Where aF is the natural gas price (3.1048 $/MMBtu from [19]), Hs is the enthalpy of saturated steam, hw is the enthalpy of boiler feedwater, and ηB is the boiler efficiency. Based on the given thermodynamic data and a boiler efficiency of 0.8, the calculated fuel cost is 4.47 $/1000 lb of steam. The total steam production cost is then estimated using [22]:

$$C_G = C_F(1 + 0.3) \qquad (2)$$

Which accounts for additional operating and maintenance expenses equal to 30% of the fuel cost. Using this approach, the final steam cost is obtained as 5.81 $/1000 lb.

Table (7): Steam requirement and operating cost of E-103 in the unmodified process.

Steam 6 bar E-103 requirement (Unmodified)	
Mass flow (kg/h)	4186.537
Mass flow (lb/h)	9229.723
Price ($/h)	53.642

As shown in Table (7), the unmodified configuration requires 4186.537 kg/h (9229.723 lb/h) of 6 bar steam, resulting in an operating cost of 53.642 $/h based on the calculated steam price. In the modified process, this steam requirement is supplied through internal waste heat recovery from high-temperature process streams, eliminating the need for equivalent external steam generation. Consequently, the steam cost incurred in the unmodified model represents direct economic savings achieved through heat integration. Overall, the results in Tables (5–7) confirm that process integration enhances both thermal efficiency and plant profitability by reducing furnace fuel consumption and external steam generation costs simultaneously.

4. Conclusions

The implementation of heat integration in the allyl chloride production process significantly improves both thermal and economic performance without altering the core reaction and separation sequence. By recovering high-temperature reactor effluent heat for propylene preheating and 6 bar steam generation, the modified configuration reduces furnace duty by 5.38×10^6 kJ/h (≈26.3%), decreases fuel consumption by 228.27 kg/h (≈26.3%), and lowers CO_2 emissions by 626.20 kg/h (≈26.3%). Furthermore, 1.3943×10^7 kJ/h of internal energy is effectively utilized to replace external steam demand, eliminating associated utility costs. The economic assessment is based on the reduction of natural gas consumption and the elimination of external steam requirements, both of which directly decrease operating expenses. Overall, the integrated design demonstrates that strategic internal heat recovery can substantially enhance energy efficiency, reduce operating costs, and improve environmental performance, thereby supporting the sustainability and competitiveness of industrial allyl chloride production.

Conflict of Interest: The authors declare that there are no conflicts of interest associated with this research project. We have no financial or personal relationships that could potentially bias our work or influence the interpretation of the results.

References

[1] Grand View Research, "Allyl chloride market size, share & trends analysis report by application (epichlorohydrin, water treatment chemicals, others), by region, and segment forecasts, 2023–2030," 2023. [Online]. Available: https://www.grandviewresearch.com/industry-analysis/allyl-chloride-market-report

[2] M. Li, L. Han, X. Luo, and H. A. Luo, "The kinetics modeling and reactor simulation of propylene chlorination reaction process," *AIChE J.*, vol. 67, no. 10, p. e17341, 2021, doi: 10.1002/aic.17341.

[3] M. Li, J. Li, H. Chen, Y. He, H. Liu, L. Han, and H. A. Luo, "Multi-objective optimization and reactor design/simulation of propylene high-temperature chlorination process utilizing the TS-EMO machine learning algorithm," *Chem. Eng. Sci.*, 2026, doi: 10.1016/j.ces.2026.123363.
[4] J. Amador, C. G. Figueroa-Cornejo, and R. A. Valencia-Fajardo, "Acercamiento a las condiciones óptimas de operación en la síntesis del cloruro de alilo," *Rev. Politécnica*, vol. 55, no. 2, pp. 107–116, 2025.
[5] Transparency Market Research, "Allyl chloride market: Global industry analysis, size, share, growth, trends, and forecast, 2019–2027," 2023. [Online]. Available: https://www.transparencymarketresearch.com/industry/chemicals-and-materials/chemicals
[6] H. Haniya, T. A. Windarti, and D. N. Paramitha, "Energy efficiency improvement through pinch analysis of gas phase chlorination process of propylene," *J. Voc. Stud. Appl. Res.*, vol. 7, no. 2, pp. 59–64, 2025, doi: 10.14710/jvsar.v7i2.30768.
[7] E. Woolley, Y. Luo, and A. Simeone, "Industrial waste heat recovery: A systematic approach," *Sustain. Energy Technol. Assess.*, vol. 29, pp. 50–59, 2018, doi: 10.1016/j.seta.2018.07.001.
[8] G. Oluleye, M. Jobson, R. Smith, and S. J. Perry, "Evaluating the potential of process sites for waste heat recovery," *Appl. Energy*, vol. 161, pp. 627–646, 2016, doi: 10.1016/j.apenergy.2015.07.011.
[9] A. P. Sánchez, A. D. L. C. G. Abad, A. A. Solares, and A. C. A. Martínez, "Simulation of an allyl chloride production process via the propylene chlorination route in ChemCAD simulator," *InGenio J.*, vol. 8, no. 1, pp. 156–173, 2025, doi: 10.18779/ingenio.v8i1.970.
[10] M. R. Flid, "The oxidative chlorination of hydrocarbons II: The oxidative chlorination of propylene, 1,3-butadiene, acetylene, and benzene," *Catalysis in Industry*, vol. 16, pp. 244–253, 2024, doi: 10.1134/S2070050424700120.
[11] M. Fomchenkov, S. Galanov, O. Sidorova, and O. Magaev, "Pyrolysis of 1,2-dichloropropane," *J. Phys.: Conf. Ser.*, vol. 1145, no. 1, p. 012046, 2019, doi: 10.1088/1742-6596/1145/1/012046.
[12] R. Turton, J. A. Shaeiwitz, and D. Bhattacharyya, *Analysis, Synthesis, and Design of Chemical Processes*, 5th ed. Boston, MA, USA: Pearson Education, 2018.
[13] G. Soave, "Equilibrium constants for modified Redlich–Kwong equation of state," *Chem. Eng. Sci.*, vol. 27, pp. 1196–1203, 1972.
[14] A. Arya, B. Maribo-Mogensen, I. Tsivintzelis, and G. M. Kontogeorgis, "Process design of industrial triethylene glycol processes using the Cubic-Plus-Association (CPA) equation of state," *Ind. Eng. Chem. Res.*, vol. 53, no. 29, pp. 11766–11778, 2014, doi: 10.1021/ie501251d.
[15] W. D. Seider, J. D. Seader, and D. R. Lewin, *Product and Process Design Principles: Synthesis, Analysis, and Evaluation*. New York, NY, USA: Wiley, 2004.
[16] U. Ibrahim and S. Farrukh, "Optimization of fuel in saturated steam boiler through preheating of controlled air-fuel mixture," in *Proc. 2019 2nd Int. Conf. Comput., Math. Eng. Technol. (iCoMET)*, 2019, pp. 1–5, doi: 10.1109/ICOMET.2019.8673398.
[17] S. Arpit and P. K. Das, "A state-of-the-art review of heat recovery steam generators and waste heat boilers," *Energy Efficiency*, vol. 16, no. 8, p. 99, 2023, doi: 10.1007/s12053-023-10179-5.
[18] J. M. Smith, H. C. Van Ness, M. M. Abbott, and M. T. Swihart, *Introduction to Chemical Engineering Thermodynamics*, 8th ed. New York, NY, USA: McGraw-Hill Education, 2018.
[19] Trading Economics, "Natural gas commodity price (Feb 2026) – Data and forecast," 2026. [Online]. Available: https://id.tradingeconomics.com/commodity/natural-gas
[20] A. T. Kirkpatrick and K. K. Kuo, *Principles of Combustion*, 3rd ed. Hoboken, NJ, USA: John Wiley & Sons, 2024.
[21] R. M. Hannun and A. H. Abdul Razzaq, "Air pollution resulted from coal, oil and gas firing in thermal power plants and treatment: A review," in *IOP Conference Series: Earth and Environmental Science*, vol. 1002, no. 1, p. 012008, Mar. 2022, doi: 10.1088/1755-1315/1002/1/012008.
[22] S. Hall, *Rules of Thumb for Chemical Engineers*. Oxford, U.K.: Butterworth-Heinemann, 2017.